Coupled simulations with SOLPS-ITER and B2.5-Eunomia for detachment experiments in Magnum-PSI

J. Gonzalez[1], R. Chandra[1,2], H. J. de Blank[1], E. Westerhof[1]

[1] DIFFER, de Zaale 20, 5612AJ, Eindhoven, The Netherlands

[2] Department of Applied Physics, Aalto University, Espoo, Finland

E-mail: `j.gonzalezmunos@differ.nl`

Abstract. Heat loads of 10 MWm^{-2} are expected for steady state operation at ITER and up to 20 MWm^{-2} in slow transient situations. Plasma linear devices like Magnum-PSI can recreate situations close as those expected to be achieved at ITER divertor, providing easier access for diagnostics than in a tokamak. Numerical models are still necessary to complement experiments and to extrapolate relevant information to fusion devices, as the relevant Atomic and Molecular (A&M) processes. SOLPS-ITER (formerly known as B2.5-Eirene) is typically employed to solve the plasma and neutral distribution in a coupled way for tokamak devices. For Magnum-PSI, B2.5 has been coupled with a different neutral module, named Eunomia, developed mostly for linear devices. Nevertheless, there is an interest in using SOLPS-ITER for simulating Magnum-PSI, as it would ease the process of relating linear device results with tokamaks. A previous work found significant differences in the implementation of relevant plasma-neutral processes in Eirene and Eunomia. A wide range of plasma scenarios are compared between B2.5-Eunomia and SOLPS-ITER. Although both codes produce results close to experimental Thomson Scattering (TS) density and temperature near the target once the electric potential at the source is adjusted, these are achieved with completely different plasma and neutral distributions. Anomalous transport coefficients, which are other of the *free-parameters* in Magnum-PSI simulation, are set equal between the two codes. When studied in a wide range of neutral pressures, SOLPS-ITER shows a trend closer to experiments, as well as providing a converged solution at neutral pressures higher than 4 Pa for which B2.5-Eunomia was unable to provide a converged solution. Additional measurements of the neutral distribution in the target chamber as well as the electric potential at the source are required to determine which code is producing results closer to the experiment.

Submitted to: *Plasma Phys. Control. Fusion*

1. Introduction

Reduction of heat and particle flux towards the divertor of a tokamak is necessary to extend the lifetime of the divertor and achieve larger operation times. The divertor target surface needs to endure heat loads that for ITER [1] will go from $10\,\mathrm{MWm^{-2}}$ in steady state operation up to $20\,\mathrm{MWm^{-2}}$ during slow transients [2]. A way to reduce these fluxes is to puff a neutral gas to achieve a detached plasma state [3, 4]. Thus, the interaction of the high energy plasma, the neutrals inside the vessel (from recombination, sputtering and gas puffing) and the wall material is of immense importance for the next generation of fusion devices. The accurate simulation and experimental characterization of plasma-neutral interactions close to the divertor's target in a tokamak is of immense importance for heat and particle control.

To study the complex interaction between plasma and target as well as the basic principles of heat and particle flux mitigation, linear devices like Magnum-PSI [5] are employed. These devices are easier and cheaper to operate and allow for better access with experimental diagnostics. Magnum-PSI can generate similar conditions to those expected to be achieved at ITER's divertor targets, reaching hydrogen flux densities of $10^{23} - 10^{25}\,\mathrm{m^{-2}s^{-1}}$ with electron and ion temperatures of $1 - 5\,\mathrm{eV}$ [6].

Nevertheless, due to the multiple challenges that arise in the plasma-surface interaction in Magnum-PSI, numerical models are required to better understand the experimental data and to validate numerical modelling against experiments. This becomes relevant for fusion detachment to extract information of the relevant Atomic and Molecular (A&M) processes taking place near the target, for example. Two numerical codes are currently being used to model Magnum-PSI: SOLPS-ITER, formerly known as B2.5-Eirene, [7, 8] and B2.5-Eunomia [9]. Both codes use the same fluid plasma solver, B2.5, coupled with a Monte-Carlo solver to obtain the neutral distribution and the plasma sources from plasma-neutral interaction, Eirene [10] and Eunomia respectively. An important endeavour has been done in developing B2.5-Eunomia and validating it against experiments [11, 12]. However, there is an intrinsic interest in using the same code for linear devices than the one used for tokamaks, as previous simulations of linear devices with SOLPS-ITER have shown [13, 14, 15].

In this work, SOLPS-ITER and B2.5-Eunomia are compared in coupled runs for a low and high neutral pressure in the target chamber to represent a detached situation. The trend of peak electron density and temperature as a function of the target chamber's neutral pressure is studied for a wide range of values. The disparate neutral distributions and sources of particles and energy obtained in the standalone comparison of Ref. [16] result in completely different plasma states. Due to the *free parameters* present in the simulation of Magnum-PSI [11], both codes are able to reach plasma profiles close to the TS experimental data a few centimetres in front of the target. This means that additional diagnostics are required to determine which code is providing results closer to the measurements.

This paper is organized as follows. Section 2 gives an overview of Magnum-PSI

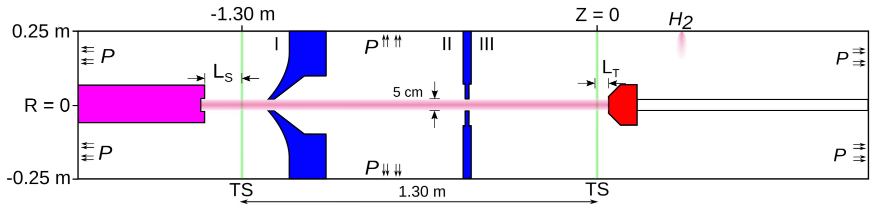

Figure 1: Simplified geometry section of Magnum-PSI. The three chambers source (I), beam dump (II) and target (III) are separated by skimmers marked in solid blue. The target position, marked in red, can be axially transposed. Figure taken with permission from Ref. [16].

and the particularities of its simulation with SOLPS-ITER and B2.5-Eunomia. Then, Sec. 3 depicts the differences between the two codes in a coupled situation. Results for two plasma scenarios, the high and low density cases from Ref. [11] in a wide range of neutral pressures, are presented in Sec. 4. Additionally, the impact of electron-molecule collision terms missing in the standard list of Eirene and Eunomia processes is included. Finally, conclusions are given in Sec. 5.

2. Simulation setup for Magnum-PSI

To study the complex interaction between plasma and target as well the basic principles of heat and particle flux mitigation, linear devices like Magnum-PSI [5, 17] can be employed [18]. This plasma linear device can generate similar conditions to those expected to be achieved at ITER's divertor targets, reaching hydrogen flux densities of $10^{23} - 10^{25}\,\mathrm{m^{-2}s^{-1}}$ with electron and ion temperatures of $1 - 5\,\mathrm{eV}$ [6]. The basic geometry of Magnum-PSI, in the cases presented in this work, is shown in Fig. 1. The main surfaces of Magnum-PSI are made of stainless-steel, which is the material used for all surfaces in the simulation except for the target, which is tungsten. Magnum-PSI is divided into three chambers separated by skimmers: source, beam dump and target, marked as I, II and III respectively. These skimmers limit the diameter of the plasma beam to around 5 cm. Moreover, the magnetic field must be large enough so the plasma beam is not too wide, which would result in an extreme head load on the first skimmer. The pressure is maintained at a specific level in each chamber thanks to the cryogenic pumps marked with P. In the target chamber, a test material, usually tungsten, is exposed to the plasma beam. A gas puff can be injected into the target chamber to increase the chamber pressure and produce a detachment plasma state. Different diagnostic are applied during a typical operation of Magnum-PSI, including Thomson Scattering (TS) near the target [19].

The main properties of the plasma close to the target and the experimental setup during the detachment experiments can be found in Tab. 1. For a more detailed analysis of the detachment experiments please refer to Ref. [11].

To simulate Magnum-PSI plasma with B2.5, a rectangular region of

	High Density	Low Density
Main plasma species	H	H
Source Chamber Pressure (Pa)	1.96	1.27
Magnetic Field (T)	1.20	1.20
Beam Dump Chamber Pressure (Pa)	0.42	0.30
Target Chamber Pressure (Pa)	$0.46 - 8.20$	$0.27 - 8.10$
Target Peak Density ($10^{20}\,\mathrm{m}^{-3}$)	$5.12 - 0.49$	$1.11 - 2.00$
Target Peak Temperature (eV)	$1.09 - 0.14$	$3.94 - 0.38$
Gas puffing in target chamber (H_2) (slm)	$0 - 12$	$0 - 12$

Table 1: Table containing the main plasma properties and relevant Magnum-PSI parameters for the detachment experiments presented here. Target pressure, electron density and temperature changed during the experiments as a function of the gas puffing at the target. The other parameters in the table remained constant.

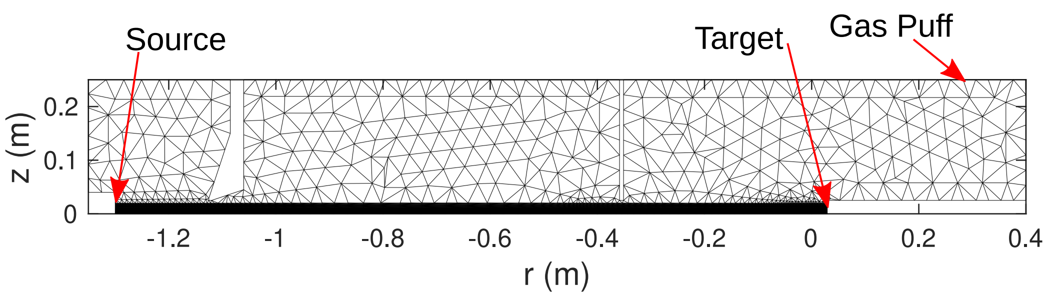

Figure 2: Eirene mesh used for the high density case in this work. The dark region at the axis represents the plasma grid. The Eunomia mesh and the meshes used for the low density case are qualitatively similar and are not shown here for the sake of simplicity.

150(axial)×36(radial) surfaces, assuming an axi-symmetrical geometry, is used to represent the plasma beam. Then, the Eirene or Eunomia grid is extended to cover the full device vessel to properly capture the dynamics of the neutrals outside the plasma region. In the plasma region, the two grids overlap so that information between plasma and neutrals can be communicated. An example of the Eirene mesh can be found in Fig. 2, in which the dark region represents the dense plasma grid. The TS target position is used as the origin ($z = 0\,\mathrm{m}$) and the plasma source is located at $z = -1.3\,\mathrm{m}$. The density and temperature profiles of TS at the source are used as boundary conditions for B2.5 assuming quasi-neutrality and equilibrium between ions and electrons.

The individual pressure in each chamber is achieved in SOLPS-ITER and B2.5-Eunomia by means of a pressure feedback loop. This loop modifies the absorption probabilities of surfaces representing Magnum-PSI's pumps to match a reference pressure, measured during the experiments.

In addition, the dynamics of neutral particles reflected by the walls of Magnum-PSI must be considered to obtain the right distribution of plasma and neutrals. Currently, it is assumed that atomic hydrogen has two possible outcomes when interacting with a Magnum-PSI wall: it is either reflected keeping its energy, with a 90% of probability, or it recombines into H_2 and it is reflected by the wall with an energy equivalent to the wall temperature [9]. Molecules are assumed to always be reflected as thermal molecules by the wall. For the plasma impacting the target, a 100% recombination is assumed, being 90% H and the remaining 10% H_2 [9]. An electrical floating target is assumed, meaning that the net current through the target is null, as it is a typical condition for Magnum-PSI experiments. The plasma reaching the edge of the beam is automatically recombined into neutrals and acts as a source of neutral particles in Eirene.

In the framework of simulating Magnum-PSI with SOLPS-ITER or B2.5-Eunomia several parameters not directly measured and used as *free parameters* have to be chosen to match the simulation output to experiments [11]. These are the electric potential profile at the source boundary condition and the transport coefficients for B2.5. For the transport coefficients, the values for Ref. [11] are employed for the simulations presented here with SOLPS-ITER and B2.5-Eunomia. The unknown electric potential, which relates with the Ohmic heating in the plasma beam, is typically fitted with a double Gaussian curve and adjusted such that the temperature at the simulated TS target position ($z = 0\,\mathrm{m}$) is in good agreement with experiment data. This hinders the predictive capability of of B2.5-Eunomia and SOLPS-ITER to simulate Magnum-PSI and increases the number of unknown parameters. Additionally, if anomalous transport coefficients are used, the electric potential profile is dependent of these values [11]. Each code requires a different electric potential profile to obtain similar electron temperature profiles in the target chamber, which directly relates to the energy exchanged with the neutrals [16]. The electric potential at the source should be measured in Magnum-PSI to obtain profiles usable in the codes, which will aid in determining which code is closer to the experiment.

3. Main differences between SOLPS-ITER and B2.5-Eunomia

It is clear that the main difference between SOLPS-ITER and B2.5-Eunomia is the use of a completely different neutral module (Eirene and Eunomia, respectively), while maintaining the same plasma solver (B2.5). Nevertheless, it should be noted that the B2.5 version used in the last B2.5-Eunomia release has not been updated to recent versions available in SOLPS-ITER. Thus, there are differences between the two plasma solvers used in each code, mostly related with bug fixes and other improvements not relevant for the cases studied here. Although these differences are barely noticeable, they should be noted as they have a small impact in the final solution. However, the big difference between the two suites is still the different implementation of plasma-neutral processes explained in Ref. [16].

The plasma grid in both codes has been set to have the same number of axial and radial elements (150×36) in the same coordinates. However, due to different processes in the grid generation for Eirene and Eunomia, neutral grids do not match, except in the plasma region, in which each B2.5 quadrilateral is divided into two triangles.

As stated in Ref. [16], Eirene and Eunomia use a different wall reflection model. Eunomia always assumes a thermal reflection of atoms and molecules. On the other hand, Eirene incorporates a *fast reflection* for atoms and thermal reflection for molecules. As the main objective of this paper is to study the standard approach of both codes for the simulation of Magnum-PSI, there has been no modification to this model. However, the probabilities of absorption, fast and thermal reflection for each species have been set equal between Eirene and Eunomia. Additionally, Eirene uses pre-calculated tables with TRIM [20, 21, 22] for the reflection model between neutrals and surfaces. These tables provide a more accurate post-reflection velocity distribution for each particle, for example to properly represent target recycling.

In this simulation regime, accounting for the transport of vibrational resolved molecules with collision rates for each vibrational states can become important [23, 24] . Eunomia can easily deal with different vibrational states for H_2 and uses the relevant collisional data from H2VIBR, as shown in Tab. 3. Although this capability can be set in Eirene, this work uses a standard approach for Eirene in which thermal equilibrium for molecules is assumed. Thus, this comparison will be performed with Eunomia tracking individual vibrational states for H_2 and Eirene assuming equilibrium. This has an impact on some collision rates [12], particularly at higher electron temperatures. Additional simulations accounting for vibrational resolved molecules in Eirene using H2VIBR will be carried out in the future to determine the impact of the distribution of vibrational levels in the simulation of Magnum-PSI.

As stated in Ref. [16], Eirene and Eunomia implement some relevant plasma-neutral collision processes in a distinct way. This leads to significant differences in the sink and sources of particles, momentum and energy passed to B2.5 to generate a new plasma scenario. The main differences appear in the implementation of Molecular Assisted Recombination (MAR), electron impact ionization (EI) of atoms and proton-molecule elastic (EL) collisions. Moreover, the standard sets of collision processes between the two codes, tables 2 and 3, present additional processes that are included or neglected in each case. It can be seen how Eirene includes two process related with H_2 that do not appear in Eunomia: dissociation ionization (AMJUEL 2.2.10) and electron impact ionization of molecules (AMJUEL 2.2.9). On the other hand, Eunomia includes processes related with the formation of H^- that aid to the recombination of protons. The impact of these missing terms in each code is analysed in sections 4.3 and 4.4, respectively.

4. Results

This section presents the main results of the comparison between SOLPS-ITER and B2.5-Eunomia in Magnum-PSI simulations. Two plasma scenarios are presented: low and high density. The plasma and neutral solutions for B2.5-Eunomia are the same as in Ref. [11]. In the high density scenario the cases have been re-run to account for the issue in double counting $p + H$ collisions [16]. For each of these plasma scenarios, two

Collision	Type	Database
$e + H \longrightarrow H^+ + 2\,e$	EI	AMJUEL 2.1.5
$H^+ + H \longrightarrow H + H^+$	CX	HYDHEL 3.1.8
$e + H_2 \longrightarrow H + H + e$	DS	AMJUEL 2.2.5g
$H + H \longrightarrow H + H$	EL	AMMONX R-H-H
$H + H_2 \longrightarrow H + H_2$	EL	AMMONX R-H-H2
$H_2 + H_2 \longrightarrow H_2 + H_2$	EL	AMMONX R-H2-H2
$H^+ + H_2 \longrightarrow H + {H_2}^+$	CX	AMJUEL 3.2.3
$e + {H_2}^+ \longrightarrow H^+ + H^+ + 2\,e$	DI	AMJUEL 2.2.11
$e + {H_2}^+ \longrightarrow H + H^+ + e$	DS	AMJUEL 2.2.12
$e + {H_2}^+ \longrightarrow H + H$	DR	AMJUEL 2.2.14
$H^+ + H_2 \longrightarrow H^+ + H_2$	EL	AMJUEL 0.3T
$e + H_2 \longrightarrow {H_2}^+ + 2\,e$	EI	AMJUEL 2.2.9
$e + H_2 \longrightarrow H + H^+ + 2\,e$	DS	AMJUEL 2.2.10
$H^+ + e \longrightarrow H(1\,s)$	RC	AMJUEL 2.1.8

Table 2: Reactions used by Eirene for atomic and molecular Hydrogen. The type of collision are: charge-exchange (CX), electron impact ionization (EI), elastic collision (EL), dissociation (DS), dissociation ionization (DI), dissociation recombination (DR) and recombination (RC).

Collision	Type	Database
$e + H \longrightarrow H^+ + 2\,e$	EI	HYDHEL 2.1.5
$e + H \longrightarrow e + H^*$	EI	HYDHEL 2.1.5
$H^+ + H \longrightarrow H + H^+$	CX	HYDHEL 3.1.8
$e + H_2 \longrightarrow H + H + e$	DS	H2VIBR 2.l1
$H^+ + e \longrightarrow H(1\,s)$	RC	AMJUEL 2.1.8
$H + H \longrightarrow H + H$	EL	Lennard-Jones
$H + H_2 \longrightarrow H + H_2$	EL	Lennard-Jones
$H_2 + H_2 \longrightarrow H_2 + H_2$	EL	Lennard-Jones
$H^+ + H_2 \longrightarrow H^+ + H_2$	EL	AMJUEL 0.3T
$H^+ + H_2(v = 0\text{-}14) \longrightarrow H + {H_2}^+$	CX	H2VIBR 2.l2
$e + {H_2}^+ \longrightarrow H + H^*$	DS	Spontaneous
$e + H_2(v = i) \longrightarrow e + H_2(v = i + 1)$	EX	H2VIBR
$e + H_2(v = i) \longrightarrow e + H_2(v = i - 1)$	DX	H2VIBR
$e + H_2(v = 0\text{-}14) \longrightarrow H + H^-$	DS	H2VIBR 2.l3
$H^- + H^+ \longrightarrow H + H^*$	RC	Spontaneous

Table 3: Reactions used by Eunomia for atomic and molecular Hydrogen. The type of collision are: charge-exchange (CX), electron impact ionization (EI), elastic collision (EL), dissociation (DS), excitation (EX), de-excitation(DX) and recombination (RC). Excited states H^* are instantaneously de-excited or ionized.

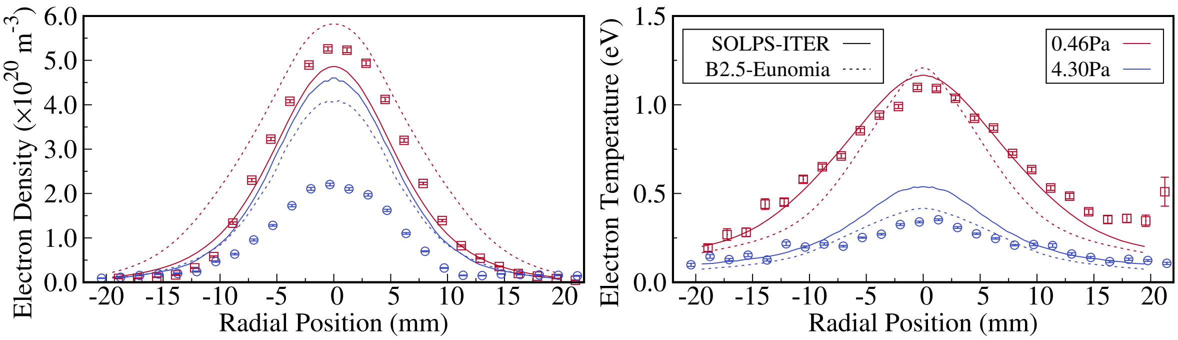

(a) Electron density (b) Electron temperature

Figure 3: Radial profiles of the electron density and temperature at the TS target position for the High Density case for two neutral pressures in the target chamber. Solid line represents SOLPS-ITER solution, dashed line is B2.5-Eunomia solution and data points are the TS measurements. Both codes produce a good agreement with experimental data, but discrepancies, particularly at the edges, still appear.

neutral pressures in the target chamber are analysed in deep. The trend of the peak temperature and density for a wide range of neutral pressures in the target chamber is also discussed. In the low pressure case, no gas puffing is included, so the neutrals in the device come only from recycling and recombination. For the high pressure case a gas puffing of H_2 is added to the simulation. This injected gas raises the pressure in the target chamber to $\sim 4\,\mathrm{Pa}$, increasing the plasma-neutral interactions and reducing the plasma flux towards the target.

4.1. High Density case

It is interesting to analyse a high density plasma scenario as this produce high flux of particles and heat as those expected at ITER divertor. The radial profile of electron density and temperature at the TS target position ($z = 0\,\mathrm{m}$) is displayed in Fig. 3. For the low pressure case (0.46 Pa) both codes produce a good agreement with experimental data, although SOLPS-ITER (solid line) is closer in density and temperature than B2.5-Eunomia (dashed line). Nevertheless, huge discrepancies between at the high pressure case appear. Experimental data show a huge reduction in both, electron temperature and density. However, simulations only capture the decrease in electron temperature. It should be mentioned that both codes use the transport coefficients and upstream boundary conditions, including the potential, for the lower pressure case.

This discrepancy in the density behaviour could be related to a miss representation of the plasma conditions at the source when a high pressure is achieved in the target chamber. As shown in Fig 4, when neutrals are puffed into the target chamber SOLPS-ITER shows a significant change in the plasma density upstream the target chamber, $z < -0.35\,\mathrm{m}$. This could mean that the source boundary conditions employed for the low pressure case are not applicable for higher pressures, as it is assumed

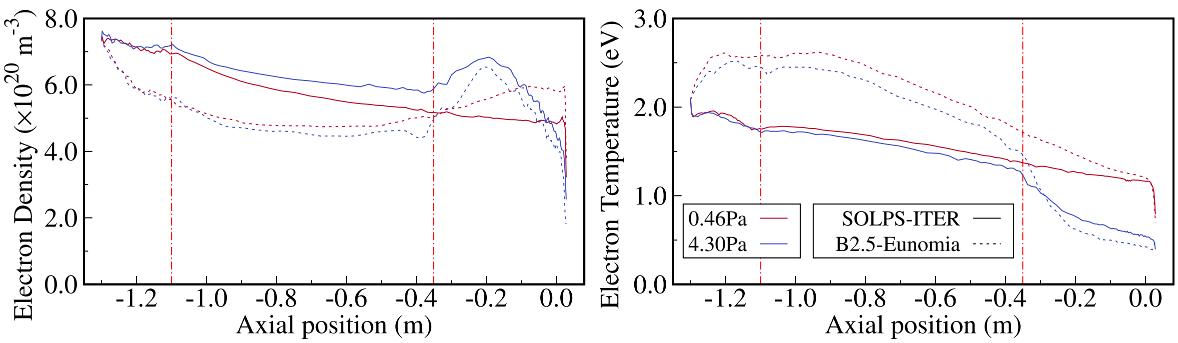

(a) Electron density (b) Electron temperature

Figure 4: Axial profiles of the electron density and temperature at $r = 0\,\mathrm{m}$ for the High Density case for two neutral pressures in the target chamber. Solid line represents SOLPS-ITER solution, dashed line is B2.5-Eunomia solution. Distinct distributions of density and temperature between the two codes appear, particularly for the high pressure case, in which plasma-neutral collisions in the target chamber become more relevant. Red dash-dotted lines represent the locations of the skimmers.

during experiments and simulations. As this upstream change is less significant in the temperature distribution, this could explain why the temperature reduction found in the simulations is closer to the experiments than the reduction in density. This should be checked experimentally in Magnum-PSI by a new series of measurements of the plasma properties near the source when high pressures are achieved at the target chamber.

Moreover, the axial distributions of Fig. 4 show a large disagreement between SOLPS-ITER and B2.5-Eunomia, even when reaching similar values at the TS target position. This indicates that it is not enough to compare at one single point as multiple distributions along the plasma beam can be achieved to match the properties at a single measurement due to the *free parameters*. Thus, experimental data should be extended to account for axial distributions, at least in small regions of the target chamber, to improve the comparison with simulations. This could be achieved in Magnum-PSI by TS measurements for different target axial positions.

Significant changes in the sources of particles and energy are found in each neutral module. Table 4 presents the sources calculated by each code for the two neutral pressure scenarios. The main difference comes from the ion and electron energy sources. B2.5-Eunomia is calculating huge sinks of plasma energy even for the low pressure case. This is directly linked to the larger amount of Ohmic heating introduced by the electric potential boundary condition at the source, needed to compensate for the energy sink. This can be seen in Fig. 5 in which the potential difference between source and target is pictured for each code. The larger amplitude in the potential is clearly shown in the B2.5-Eunomia case, which results in a larger amount of Ohmic heating. The differences in energy sources can be traced to the different implementation of $\mathrm{p} + \mathrm{H}_2$ elastic collision and MAR explained in Ref. [16]. These processes are the next significant ones in the

	0.46Pa		4.30Pa		$\Delta(0.46-4.30)$Pa	
	SOLPS-ITER	B2.5-Eunomia	SOLPS-ITER	B2.5-Eunomia	SOLPS-ITER	B2.5-Eunomia
Electron Energy (W)	-543.92	-282.83	-471.33	-186.35	-72.59	-96.48
Ion Energy (W)	-30.97	-1259.50	-271.40	-1470.02	240.43	210.52
Ion particle (part/s)	-1.94e20	-2.22e20	-5.24e20	-5.68e20	3.30e20	3.46e20

Table 4: Integrated sources for electron energy, ion energy and ion particles for the high density case. Last two columns represent the change from the low pressure to the high pressure case. Although the sources calculated by the two neutral modules are quite different, the change between the low and the high pressure case are quite close.

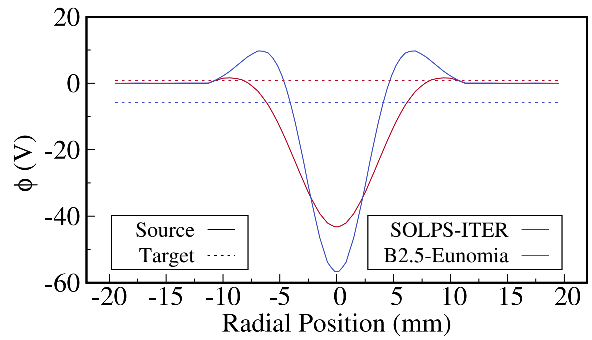

Figure 5: Potential difference between the source (solid line) and the target (dashed line) for the high density case. Curves have been shifted to have a common value of 0 V at the edge for plotting purposes.

electron energy losses after recombination [12].

Nevertheless, looking at the variation between the low and high pressure cases, last two columns in Tab. 4, similar values are achieved. The similarity in ion particle source is directly related with MAR and EI not being significant processes in this plasma scenario [12] as recombination dominates, which is implemented in the same way by Eirene and Eunomia [16].

As both neutral modules implement relevant plasma-neutral collision process differently [16], it is expected that the final distribution of neutrals also differs. The main difference can be found in the distribution of atomic hydrogen, presented in Fig. 6. B2.5-Eunomia is computing neutral densities of H in the plasma beam that are almost one order of magnitude higher than SOLPS-ITER, although the resulting temperatures are in good agreement between the two codes. On the other hand, differences in H_2 distribution, presented in Fig. 7, are smaller. Density produced by Eirene and Eunomia seems much closer than for the atomic case and both codes indicate that molecules are the dominant neutral species in that position of the plasma beam. However, a higher temperature of H_2 is being obtained by Eirene than by Eunomia close to the plasma peak ($r \leq 5$ mm). This is directly related with $p + H_2$ being the dominant plasma-molecule process in this plasma scenario [12] which gives higher molecular temperatures in Eirene [16].

The comparison between the two codes and experimental data for a wider range

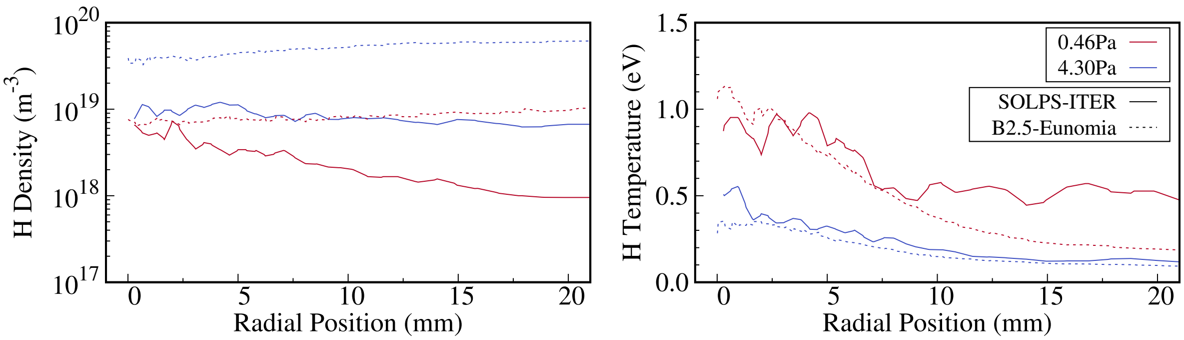

(a) H density (b) H temperature

Figure 6: Radial profiles of the atomic hydrogen density and temperature at the TS target position for the High Density case for two neutral pressures in the target chamber. Solid line represents SOLPS-ITER solution, dashed line is B2.5-Eunomia solution.

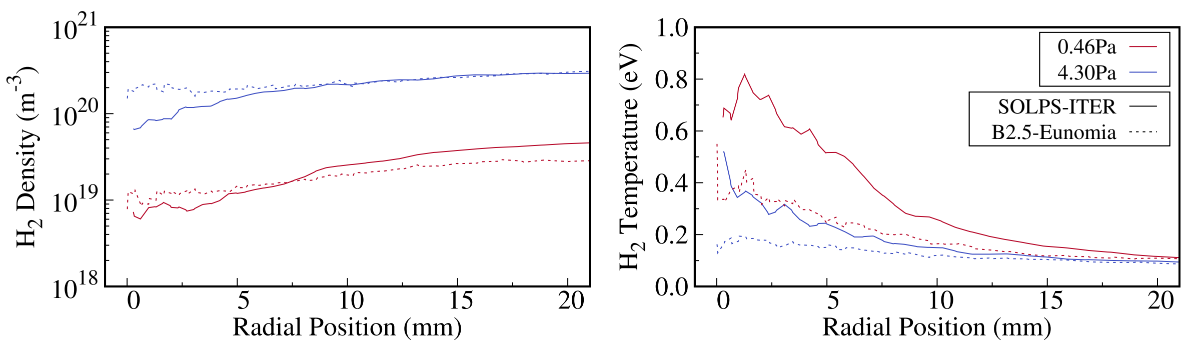

(a) H_2 density (b) H_2 temperature

Figure 7: Radial profiles of the molecular hydrogen density and temperature at the TS target position for the High Density case for two neutral pressures in the target chamber. Solid line represents SOLPS-ITER solution, dashed line is B2.5-Eunomia solution.

of neutral pressures in the target chamber is presented in Fig. 8. The temperature measured by means of TS decreases as pressure in the target chamber increases. Density remains constant for low pressures decreases for neutral pressures above 4 Pa as the incoming plasma recombines due to the high presence of neutrals. As the plasma is low temperature even at low neutral pressures, ionization has a small role and most of the plasma-neutral exchange comes from elastic interactions, charge-exchange and recombination [12]. Both codes produce a good agreement in the electron temperature but fail to capture the dependence of the electron density. It seems that SOLPS-ITER is better in producing a match with the density trend as it does not show the increase in electron density found in B2.5-Eunomia. SOLPS-ITER is able to run cases in which the pressure at the target chamber is larger than 4 Pa, in which B2.5-Eunomia fails to reach a converged state mostly due to the large sink of energy calculated by Eunomia or the computational time required to reach it is prohibitively long due to trapped particles.

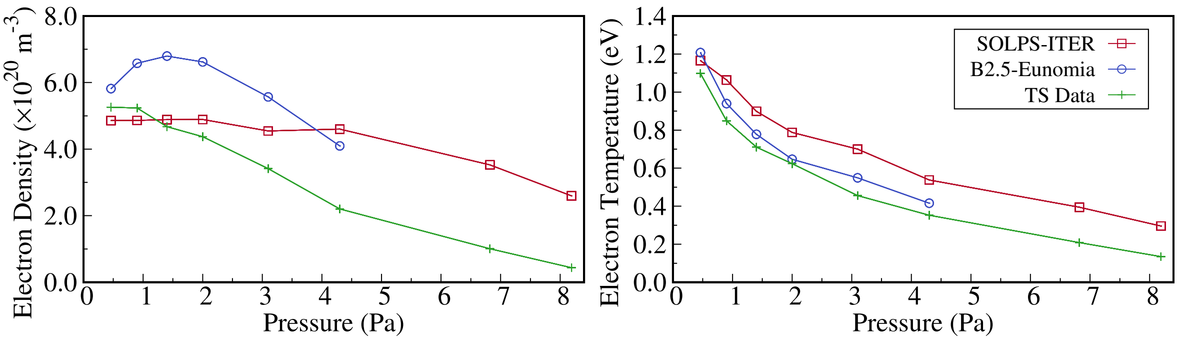

(a) Peak electron density (b) Peak electron temperature

Figure 8: Electron peak density (left) and temperature (right) at the TS target position. Discrepancies between the two codes and experimental data still appear, particularly for the electron density. However, SOLPS-ITER is capable of simulating a wider range of neutral pressures.

Although the agreement is still not good, it seems that SOLPS-ITER improves the representation of the HD case with respect to B2.5-Eunomia.

4.2. Low Density case

In this plasma scenario, Magnum-PSI achieves higher temperatures in the target chamber, but lower densities. This has a significant impact in the collisional rates, meaning that the set of relevant A&M processes changes [12]. Thus, it is important to analyse the different results obtained with SOLPS-ITER and B2.5-Eunomia in order to characterize these differences.

Figure 9 presents the radial profile of electron density and temperature at the TS target position. Both codes produce results that are in good agreement with the experimental data shown, both in density and temperature. However, the shape of the profiles is not completely recovered by any code, particularly in the case of the density. This could be related with the anomalous transport coefficients employed, which affect the shape of the profile. This is more noticeable in SOLPS-ITER, as it is using the transport coefficients adapted from a B2.5-Eunomia solution instead of finding a new set that better fit the TS data. It could be possible that a different set of transport coefficients provides a better match between SOLPS-ITER and experimental data. This remarks the relevance of having independent kinetic simulations or experimental measurements that provide an approximate value for these parameters.

Although both codes are in good agreement with experimental data, this is achieved with different axial distributions of plasmas, as shown in Fig. 10, particularly for the case of 4.30 Pa. As anomalous transport coefficients are the same in both simulations, these differences must be related to the electric potential at the source and the different implementation of plasma-neutral processes in the two neutral modules. The different implementation of these processes leads to disparate sinks and sources of particles and

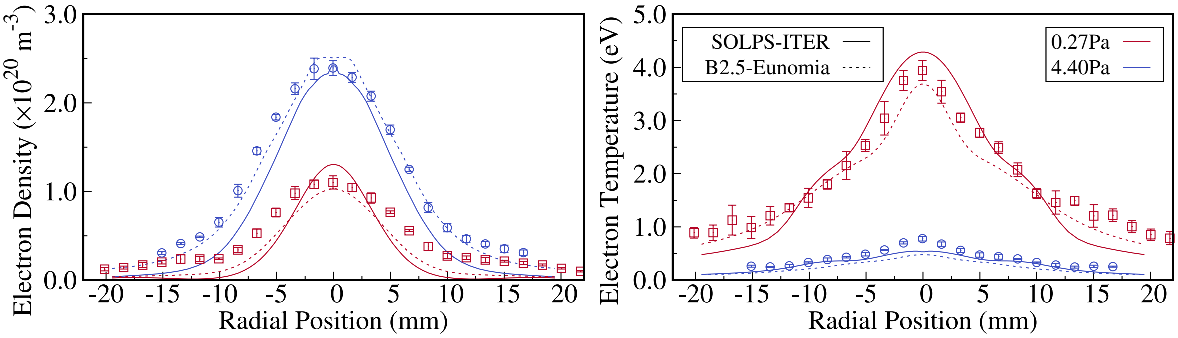

(a) Electron density (b) Electron temperature

Figure 9: Radial profiles of the electron density and temperature at the TS target position for the Low Density case for two neutral pressures in the target chamber. Solid line represents SOLPS-ITER solution, dashed line is B2.5-Eunomia solution and data points are the TS measurements. Both codes produce a good agreement with experimental data, but discrepancies, particularly at the edges, still appear.

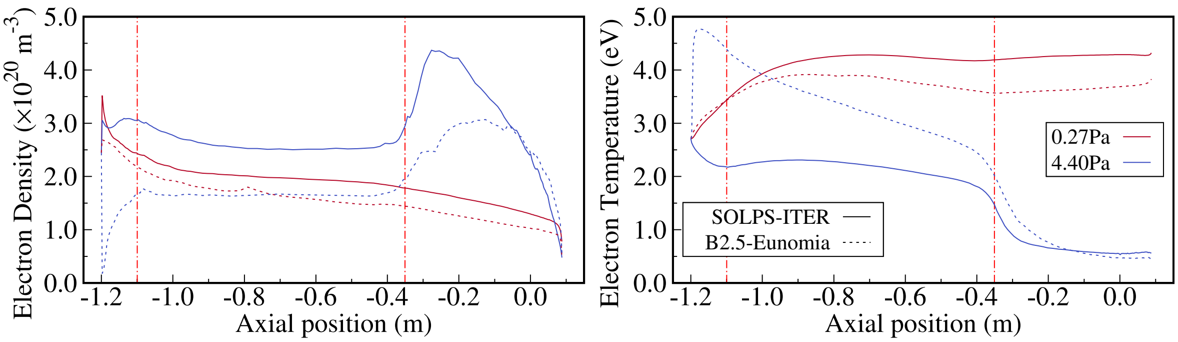

(a) Electron density (b) Electron temperature

Figure 10: Axial profiles of the electron density and temperature at $r = 0\,\mathrm{m}$ for the Low Density case for two neutral pressures in the target chamber. Solid line represents SOLPS-ITER solution, dashed line is B2.5-Eunomia solution. Disparate distributions of density and temperature between the two codes appear, particularly for the high pressure case, in which plasma-neutral collisions in the target chamber become more relevant. Red dash-dotted lines represent the locations of the skimmers.

energy [16], as can be seen in Tab. 5 for this case. At low pressure, the two codes produce behaviours completely disparate. A positive source of ions appears for SOLPS-ITER, meaning that ionization is larger than recombination. Moreover, B2.5-Eunomia estimates almost twice the energy loss by the ions in the plasma beam, as well as two times the values of the change in ion energy from the low pressure to the high pressure case. This can be explained by MAR becoming a relevant plasma-neutral collision process in this plasma scenario [12], which has a significant different implementation in Eirene and Eunomia, producing disparate sources of particles and energy [16].

	0.27Pa		4.40Pa		$\Delta(0.27 - 4.40)$Pa	
	SOLPS-ITER	B2.5-Eunomia	SOLPS-ITER	B2.5-Eunomia	SOLPS-ITER	B2.5-Eunomia
Electron Energy (W)	558.42	-301.13	288.07	-292.09	270.35	-9.04
Ion Energy (W)	-414.84	-901.34	-536.52	-1115.70	121.68	214.39
Ion particle (part/s)	1.59e19	-4.64e19	-1.20e20	-1.56e20	1.36e20	1.10e20

Table 5: Integrated sources for electron energy, ion energy and ion particles for the low density case. B2.5-Eunomia produces larger sinks of ion and electron energy, which means that a higher Ohmic heating is needed to reach the same temperature at the TS target position. Last two columns represent the change from the low pressure to the high pressure case.

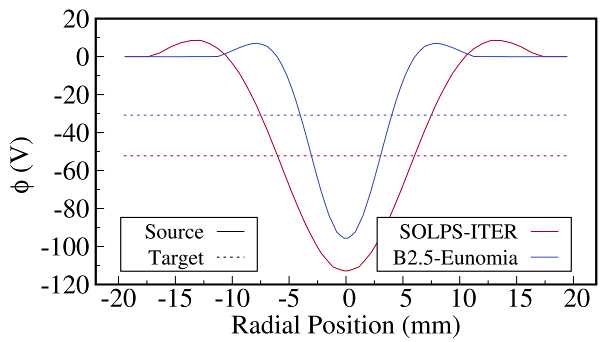

Figure 11: Potential difference between the source (solid line) and the target (dashed line) for the low density case. Curves have been shifted to have a common value of 0 V at the edge for plotting purposes.

Both codes achieve temperatures at the TS target position close to the experimental data due to the different electric potential imposed as a boundary condition at the source, as shown in Fig. 11. It is clear that B2.5-Eunomia imposes to the plasma a much larger potential drop between source and target, which will result in a larger amount of Ohmic heating. Experimental data of the potential near the source will help to determine which input of Ohmic heating is closer to Magnum-PSI scenario.

Additionally, the distribution of neutrals calculated by each neutral module differs. Figure 12 depicts the radial profile of atomic hydrogen at the TS position. For the low density case, SOLPS-ITER calculates that the temperature of H in the plasma beam is two times the one in B2.5-Eunomia and density decays with a higher rate. On the other hand, for the 4.40 Pa case, there is a huge difference of one order of magnitude in H density while temperatures are quite similar. The difference in neutral distributions can also be appreciated for the molecular hydrogen, as shown in Fig. 13. Although far from the plasma beam similar distribution of molecular density and temperature are achieved, SOLPS-ITER presents higher temperatures and lower densities for $r < 5$ mm. The higher temperatures computed in SOLPS-ITER for H and H_2 indicate a strong effect of plasma-molecule interactions due to the higher electron temperature than in the High Density scenario.

A significant difference can be appreciated if a larger number of target pressure

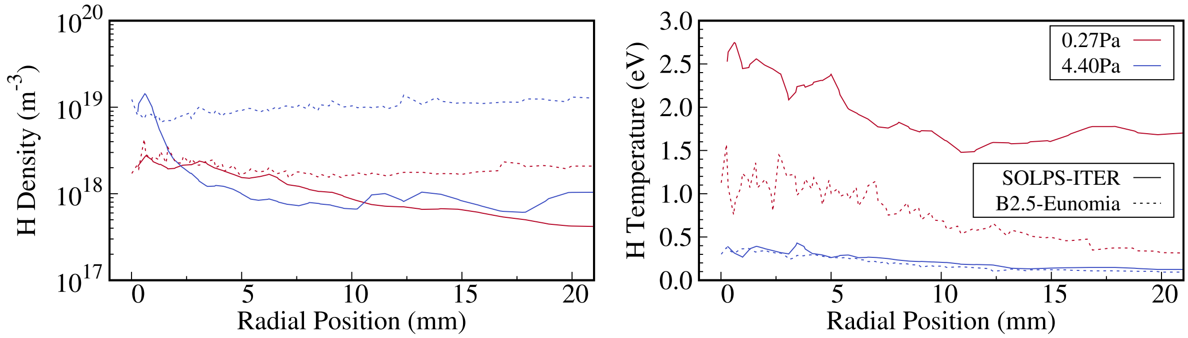

(a) H density (b) H temperature

Figure 12: Radial profiles of the atomic hydrogen density and temperature at the TS target position for the Low Density case for two neutral pressures in the target chamber. Solid line represents SOLPS-ITER solution, dashed line is B2.5-Eunomia solution.

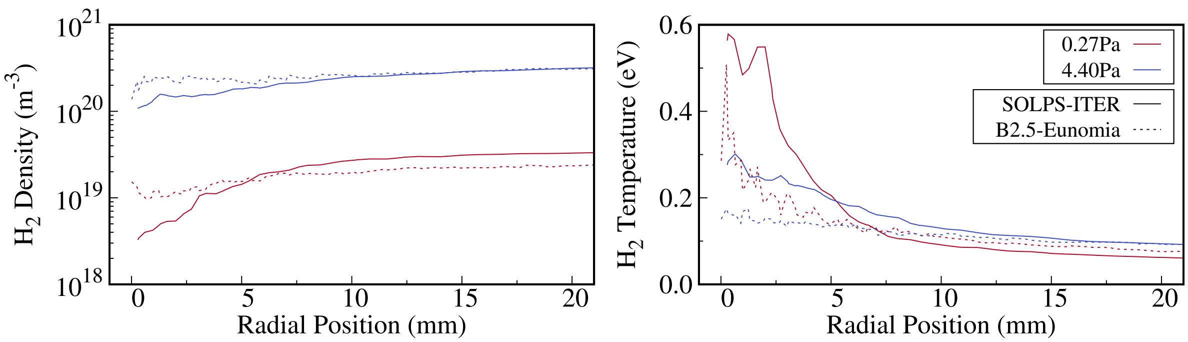

(a) H_2 density (b) H_2 temperature

Figure 13: Radial profiles of the electron density and temperature at the TS target position for the Low Density case for two neutral pressures in the target chamber. Solid line represents SOLPS-ITER solution, dashed line is B2.5-Eunomia solution and data points are the TS measurements. Both codes produce a good agreement with experimental data, but discrepancies, particularly at the edges, still appear.

scenarios is studied. Figure 14 presents the peak temperature and density at the TS target position compared with the experimental data. As with the high density case, the electron temperature reduces drastically as pressure is increased due to H_2 puffing. Electron density raises as ionization is a relevant process for this plasma scenario. However, for $P > 4\,\mathrm{Pa}$ electron density reduces in both, TS data and SOLPS-ITER simulations. SOLPS-ITER is capable of simulating higher pressures in the target chamber than B2.5-Eunomia, as in the HD case. Moreover, an improved agreement is found in the evolution of the electron density in SOLPS-ITER with respect to B2.5-Eunomia, particularly for low neutral pressures, although discrepancies appear at 8 Pa. Thus, SOLPS-ITER is better in capturing the plasma behaviour at a wider range of neutral pressures also for low density plasma scenarios.

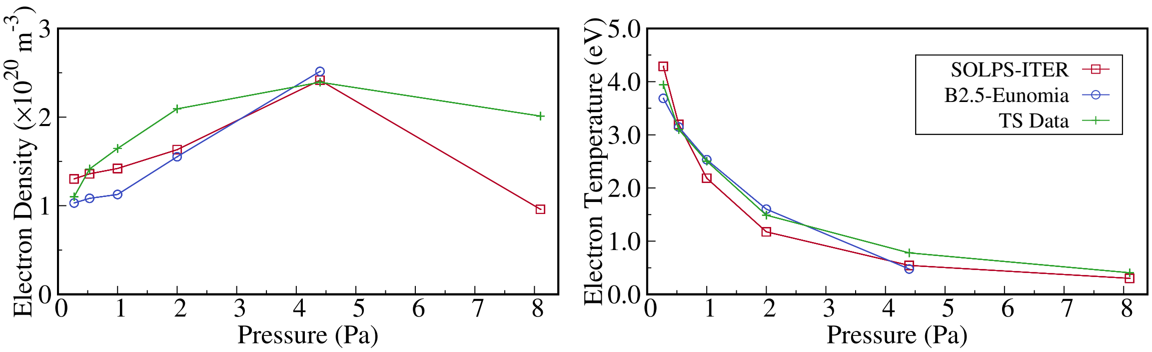

(a) Peak electron density

(b) Peak electron temperature

Figure 14: Electron peak density (left) and temperature (right) at the TS target position. In general, SOLPS-ITER has a better agreement than B2.5-Eunomia and it is able to simulate higher pressures in which B2.5-Eunomia reaches convergence issues.

4.3. Effect of missing molecule collision processes in Eunomia

From studying tables 2 and 3, it can be seen that the two codes implement quite different set of processes. Particularly relevant are the electron impact ionization of molecules (AMJUEL 2.2.9) and the dissociation ionization (AMJUEL 2.2.10) missing in Eunomia. Although the impact of these processes might be small due to a reduced collision rate, there might be situations in which they have a significant impact, *i.e.*, at high electron temperatures.

To test the impact of these processes, a series of cases in SOLPS-ITER switching these collisions is presented in Fig. 15. Taking as a base case the low density solution presented in Sec. 4.2, two additional cases are introduced: without the dissociation ionization and without electron impact ionization of molecules. The dissociation ionization (AMJUEL 2.2.10) seems to have very little effect in the plasma distribution for this regime. However, the electron impact ionization (AMJUEL 2.2.9) produces a significant sink of energy in the plasma, thus increasing the plasma temperature when it is not accounted for. This means that neglecting this process is underestimating the plasma-neutral interactions in situations when electron temperatures are above 3 eV, as typically happens in Magnum-PSI plasma beam, particularly at the peak.

Thus, collisional processes, even neglected at first due to low collision rate, might have a significant impact in simulations of Magnum-PSI. Additionally, this will affect the free parameters, mostly source potential and transport coefficients, needed to match experimental data. Additionally, these processes could have a larger impact in the divertor leg as electron temperatures upstream are usually higher than those achieved in Magnum-PSI.

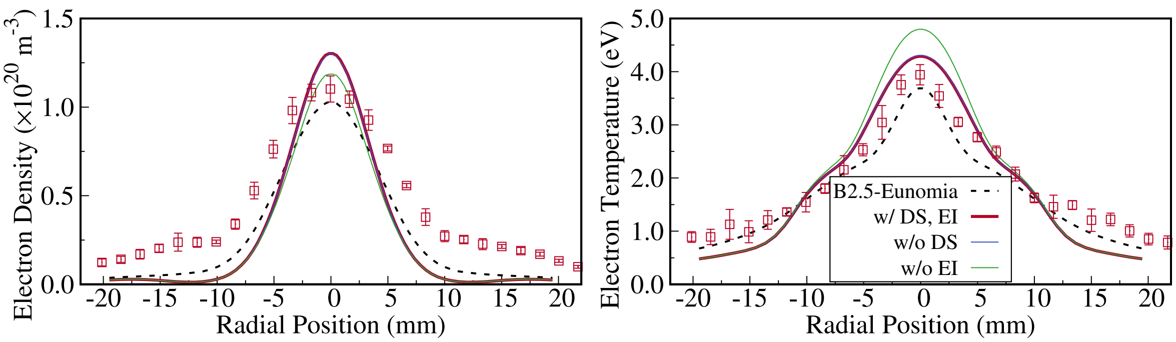

(a) Electron density (b) Electron temperature

Figure 15: Effect of missing molecule processes in Eunomia. The SOLPS-ITER solution is presented with a dashed black line. Thomson Scattering measurements at the same position as simulation profiles are shown as data points. SOLPS-ITER solutions for three cases are presented: the base case from Sec. 4.2, without ionization of molecules by electron impact (without EI) and without the dissociation ionization process (without DS) The dissociation ionization (DS) seems to have very little impact in the final solution. However, when ionization of H_2 by electron impact is neglected, a significant increase in the plasma temperature appears.

4.4. Effect of missing molecule collision processes in Eirene

This section analyses the impact of MAR via H^- (H2VIBR 2.l3) in Eunomia as this is missing in SOLPS-ITER default set of collision processes for H_2. The H^- generated by this collision process instantaneously recombines with a proton, so it could be an important process for plasma recombination particularly for high H_2 densities.

Figure 16 depicts the main collision processes involving H_2 and ${H_2}^+$. The main collision process taking place for a neutral molecule is elastic interactions with protons. However, other outcomes are possible: either a molecule is ionized (due to CX or EI) or it gets dissociated into H and H^-. The first option is more probable at $T > 0.7\,\mathrm{eV}$, in which then the ionized molecule will dissociate (DS) or dissociate and recombine (DR) depending on the electron density and temperature. For temperatures below 0.7 eV, the dominant electron-molecule collisional process is MAR via H^-, which is missing in the Eirene standard list of processes. Although this process collision rate is lower than the elastic exchange for these temperatures [23, 25], it might produce small changes in the plasma distributions in low temperature high molecule density scenarios as the high neutral pressure cases presented here.

Figure 17 presents the electron density and temperature for B2.5-Eunomia simulations with and without accounting for H^- for the high density case presented in Sec. 4.1 at 4.30 Pa. Although the effect of MAR via H^- is small, neglecting it produces higher temperatures and densities as in SOLPS-ITER. Thus, the description of plasma at low temperatures and high molecular density could be slightly improved by the implementation of this recombination process. However, as changes are small, this

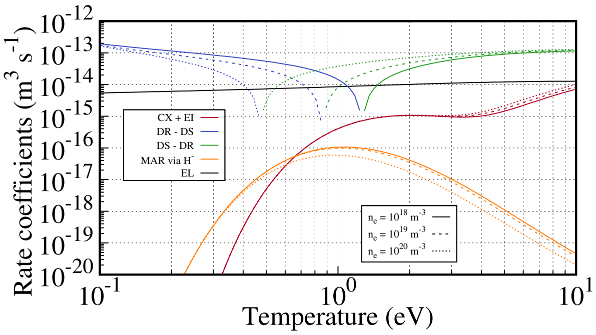

Figure 16: Collision processes involving H_2 and ${H_2}^+$ for the relevant range of temperatures and densities in Magnum-PSI. The main collision process in Magnum-PSI is $p + H_2$ elastic interaction. If a molecule assists in a recombination process the path of H^- (orange line) is more probable at $T < 0.7\,\mathrm{eV}$. If an ionized molecule is formed, the outcome of the dissociation recombination (DR) or simply dissociation (DS) strongly depends on the electron density and temperature. For higher temperatures, charge-exchange and ionization dominate, and the dissociation (DS) of ${H_2}^+$ becomes the dominant process.

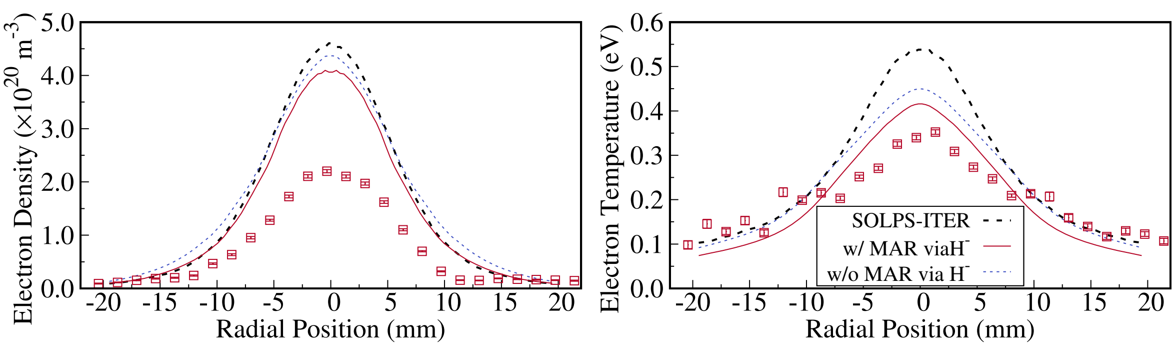

(a) Electron density

(b) Electron temperature

Figure 17: Effect of missing molecule processes in Eirene. The SOLPS-ITER solution is presented with a dashed black line for reference. Thomson Scattering measurements at the same position are shown as data points. Neglecting MAR via H^- makes B2.5-Eunomia produce results closer to SOLPS-ITER, meaning that this process slightly improves the description of plasma at low electron temperature and high molecular density.

collisional process cannot be responsible of the discrepancies found between simulations and TS.

This process has been added to the Eirene set of collisions with a combination of

$$\mathrm{e} + H_2 \longrightarrow H + H^- \qquad \text{AMJUEL 2.2.17}$$
$$H^+ + H^- \longrightarrow H + H \qquad \text{AMJUEL 7.2.3a}$$

An additional non-tracked ion species in Eirene to represent H^- has been added, the

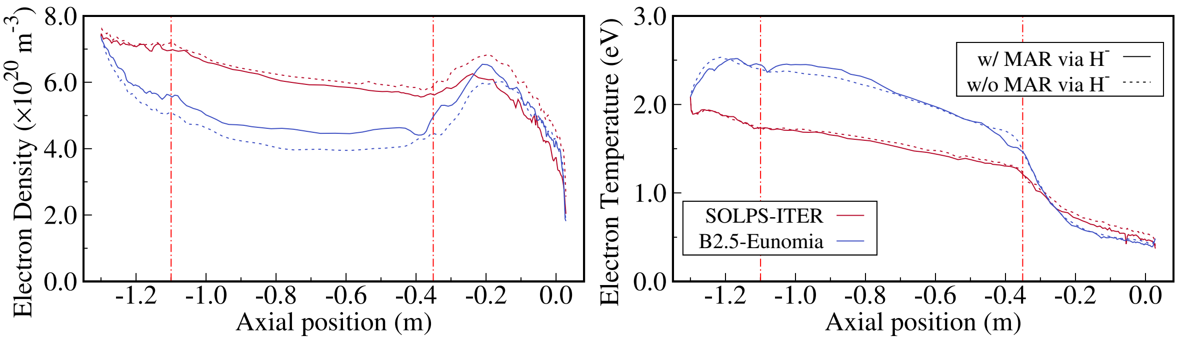

(a) Electron density

(b) Electron temperature

Figure 18: Axial distributions of electron density (left) and temperature (right) for SOLPS-ITER (red) and B2.5-Eunomia (blue) with (solid line) and without (dashed line) MAR via H^-. Red dash-dotted lines represent the locations of the skimmers. Larger change in plasma distribution occurs in the target chamber, when the population of molecules is higher.

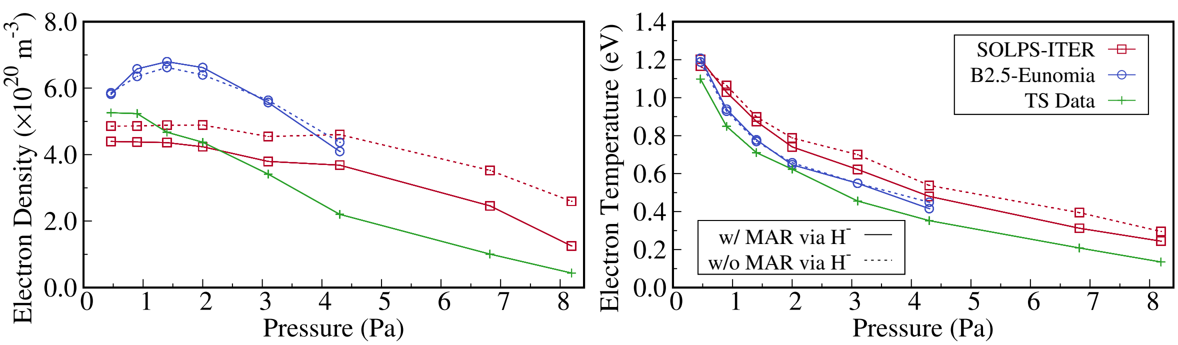

(a) Peak electron density

(b) Peak electron temperature

Figure 19: Electron peak density (left) and temperature (right) at the TS target position. Simulations with MAR via H^- are shown in solid line while the dashed lines represents the simulations without. SOLPS-ITER shows a larger impact on the plasma distribution than B2.5-Eunomia.

same way as H_2^+ is incorporated.

Particles from this species recombine immediately with a proton as a significant population of H^- in the plasma beam is not expected to exists for large periods of time. Figure 18 shows the axial distribution of the high density case at 4.30 Pa for SOLPS-ITER and B2.5-Eunomia with and without MAR via H^-. The main effect of this process for SOLPS-ITER is found in the target chamber, where the density of molecules is larger. The main impact appears in the electron density, while temperatures remain basically unaffected. This is also appreciated in the evolution of the temperature and density peaks for a wide range of pressures in Fig. 19.

5. Conclusions

This work presents a comparison of SOLPS-ITER and B2.5-Eunomia coupled runs in the framework of Magnum-PSI detachment experiments for two plasma scenarios: High and Low density. A previous work [16] studied the effect of different implementations of plasma-neutral interactions employed by each neutral module, Eirene and Eunomia. That analysis showed large discrepancies between the sources of energy and particles that will be used by B2.5 to compute a new plasma state. Here, the effect of these differences is analysed in a complete coupled run. Two neutral pressures in the target chamber are acutely analysed to represent an attached (low pressure without gas puffing) and detached (high pressure with gas puffing) situations.

The main impact of these differences is that each code requires a different boundary condition profile for the electric potential at the plasma source. This profile determines the Ohmic heating in the plasma beam, which directly impacts the plasma temperature at the target. Thus, this potential profile is modified so that simulations match the temperature profile at the TS target position. In general, B2.5-Eunomia requires a larger amount of Ohmic heating because Eunomia is computing larger sinks of plasma energy.

After modifying this electric potential at the source both codes produce similar results at the TS target position, but large differences in the plasma axial distribution appear. As transport coefficients are set equal in both codes, this can only be compensated by the source electric potential boundary condition. Moreover, disparate distributions of neutrals in the target chamber are computed by each code. Particularly significant differences are found in the distribution of atomic hydrogen density, which vary by one order of magnitude between the two codes. A qualitatively comparison with experimental data of the distribution of atomic hydrogen would provide a better understanding on which code is producing results closer to the experiment.

The sources of energy and particles computed by each neutral module are completely different in each case. Some agreement can be found at the high density case for the particle source of protons as both codes produce similar results. Moreover, the variation from the low to the high pressure in the HD case is basically the same for SOLPS-ITER and B2.5-Eunomia, although the values for each case are completely different. Nevertheless, this similitude does not translate to the low density case, in which changes in the sources show significant differences. This can be directly traced to the different implementation of MAR, which has a significant contribution in the LD scenario [12]. The effect of vibrational state distributions in these cases should be further investigated, taking advantage of new developments of Collisional Radiative Models [26].

Even when a good agreement is found with experimental TS data, differences still appear, particularly at the HD case. The codes do not properly reproduce the reduction in electron density at 4.30 Pa found experimentally. B2.5-Eunomia seems to produce a larger reduction in density and temperature than SOLPS-ITER but does not improve the solution significantly. The cause of this is still unclear and further analysis when new experimental data is available should be carried out.

SOLPS-ITER is able to obtain a converged solution in a wider range of neutral pressures than B2.5-Eunomia. Moreover, the trend of peak density and temperature as a function of the pressure has a qualitatively better match to experimental data in SOLPS-ITER. This could indicate that the implementation of plasma-neutral collision terms is more adequate in Eirene than in Eunomia for simulating plasma in the parameter range presented here. Nevertheless, additional experiments are still required to determine which code is producing more accurate results. Particularly important are the electric potential at the source and the distribution of neutral particles in the target chamber.

In this comparison, the effect of missing collision terms in the *standard* input configuration of each code were analysed. In B2.5-Eunomia, the electron impact (EI) ionization and the dissociation ionization of H_2 are not taking into account. An analysis with SOLPS-ITER shows a significant effect of EI ionization for the low density case, where electron temperatures are higher. On the other hand, the recombination of H^+ assisted by molecule through H^- implemented in Eunomia and missing in Eirene has a small effect in the plasma distribution. The implementation of this process in Eirene would slightly improve the description of plasma at low temperature and high molecular density.

Acknowledgments

This work has been carried out within the framework of the EUROfusion Consortium, funded by the European Union via the Euratom Research and Training Programme (Grant Agreement No 101052200 — EUROfusion). Views and opinions expressed are however those of the author(s) only and do not necessarily reflect those of the European Union or the European Commission. Neither the European Union nor the European Commission can be held responsible for them. The general development of EIRENE goes within EUROFusion E-TASC TSVV-5 project. This work was carried out on the Dutch national e-infrastructure with the support of SURF Cooperative and the EUROfusion High Performance Computer Marconi-Fusion hosted at Cineca (Bologna, Italy). This work is part of the research programme "The Leidenfrost divertor: a lithium vapour shield for extreme heat loads to fusion reactor walls" with project number VI.Vidi.198.018, which is (partly) financed by NWO.

References

[1] H Bolt, V Barabash, G Federici, J Linke, A Loarte, J Roth, and K Sato. Plasma facing and high heat flux materials–needs for iter and beyond. *Journal of Nuclear Materials*, 307:43–52, 2002.

[2] JP Gunn, S Carpentier-Chouchana, F Escourbiac, T Hirai, S Panayotis, RA Pitts, Y Corre, R Dejarnac, M Firdaouss, M Kočan, et al. Surface heat loads on the iter divertor vertical targets. *Nuclear Fusion*, 57(4):046025, 2017.

[3] M Wischmeier, M Groth, A Kallenbach, AV Chankin, DP Coster, R Dux, A Herrmann, HW Müller,

R Pugno, D Reiter, et al. Current understanding of divertor detachment: Experiments and modelling. *Journal of nuclear materials*, 390:250–254, 2009.

[4] VA Soukhanovskii, R Maingi, CE Bush, R Raman, RE Bell, R Kaita, HW Kugel, CJ Lasnier, BP LeBlanc, JE Menard, et al. Divertor heat flux reduction and detachment experiments in nstx. *Journal of nuclear materials*, 363:432–436, 2007.

[5] G De Temmerman, MA Van Den Berg, J Scholten, A Lof, HJ Van Der Meiden, HJN Van Eck, TW Morgan, TM De Kruijf, PA Zeijlmans Van Emmichoven, and JJ Zielinski. High heat flux capabilities of the magnum-psi linear plasma device. *Fusion Engineering and Design*, 88(6-8):483–487, 2013.

[6] H.J.N. van Eck, G.R.A. Akkermans, S. Alonso van der Westen, D.U.B. Aussems, M. van Berkel, S. Brons, I.G.J. Classen, H.J. van der Meiden, T.W. Morgan, M.J. van de Pol, J. Scholten, J.W.M. Vernimmen, E.G.P. Vos, and M.R. de Baar. High-fluence and high-flux performance characteristics of the superconducting magnum-psi linear plasma facility. *Fusion Engineering and Design*, 142:26–32, 2019.

[7] Sven Wiesen, Detlev Reiter, Vladislav Kotov, Martine Baelmans, Wouter Dekeyser, AS Kukushkin, SW Lisgo, RA Pitts, Vladimir Rozhansky, Gabriella Saibene, et al. The new solps-iter code package. *Journal of nuclear materials*, 463:480–484, 2015.

[8] Detlev Reiter, Martine Baelmans, and Petra Boerner. The eirene and b2-eirene codes. *Fusion science and technology*, 47(2):172–186, 2005.

[9] RC Wieggers, DP Coster, PWC Groen, HJ De Blank, and WJ Goedheer. B2. 5-eunomia simulations of pilot-psi plasmas. *Journal of Nuclear Materials*, 438:S643–S646, 2013.

[10] Dmitriy V Borodin, Friedrich Schluck, Sven Wiesen, DM Harting, Petra Boerner, Sebastijan Brezinsek, Wouter Dekeyser, Stefano Carli, Maarten Blommaert, Wim Van Uytven, et al. Fluid, kinetic and hybrid approaches for neutral and trace ion edge transport modelling in fusion devices. *Nuclear Fusion*, 2021.

[11] Ray Chandra, HJ De Blank, P Diomede, HJN Van Eck, HJ Van Der Meiden, TW Morgan, JWM Vernimmen, and Egbert Westerhof. B2. 5-eunomia simulations of magnum-psi detachment experiments: I. quantitative comparisons with experimental measurements. *Plasma Physics and Controlled Fusion*, 63(9):095006, 2021.

[12] Ray Chandra, Hugo J de Blank, Paola Diomede, and Egbert Westerhof. B2. 5-eunomia simulations of magnum-psi detachment experiments: Ii. collisional processes and their relevance. *Plasma Physics and Controlled Fusion*, 2021.

[13] Margarita Baeva, WJ Goedheer, NJ Lopes Cardozo, and D Reiter. B2-eirene simulation of plasma and neutrals in magnum-psi. *Journal of nuclear materials*, 363:330–334, 2007.

[14] Juergen Rapp, Larry W Owen, John Canik, Jeremy D Lore, Juan F Caneses, Nischal Kafle, H Ray, and M Showers. Radial transport modeling of high density deuterium plasmas in proto-mpex with the b2. 5-eirene code. *Physics of Plasmas*, 26(4):042513, 2019.

[15] Michele Sala, Elena Tonello, Andrea Uccello, Xavier Bonnin, Daria Ricci, David Dellasega, Gustavo Granucci, and Matteo Passoni. Simulations of argon plasmas in the linear plasma device gym with the solps-iter code. *Plasma Physics and Controlled Fusion*, 62(5):055005, 2020.

[16] Jorge Gonzalez, R Chandra, Hugo J de Blank, and Egbert Westerhof. Comparison between solps-iter and b2. 5-eunomia for simulating magnum-psi. *Plasma Physics and Controlled Fusion*, 2022.

[17] MJ van de Pol, S Alonso van der Westen, DUB Aussems, MA van den Berg, S Brons, HJN van Eck, GG van Eden, HJW Genuit, HJ van der Meiden, TW Morgan, et al. Operational characteristics of the superconducting high flux plasma generator magnum-psi. *Fusion Engineering and Design*, 136:597–601, 2018.

[18] R Perillo, Ray Chandra, GRA Akkermans, IGJ Classen, SQ Korving, and Magnum-PSI Team. Investigating the effect of different impurities on plasma detachment in linear plasma machine magnum-psi. *Physics of Plasmas*, 26(10):102502, 2019.

[19] GJ Van Rooij, HJ Van der Meiden, WR Koppers, AE Shumack, WAJ Vijvers, J Westerhout,

GM Wright, J Rapp, et al. Thomson scattering at pilot-psi and magnum-psi. *Plasma Physics and Controlled Fusion*, 51(12):124037, 2009.

[20] G Bateman. Distribution of neutrals scattered off a wall. *PPPL Appl. Phys. Rep*, 1, 1980.

[21] Wolfgang Eckstein. *Computer simulation of ion-solid interactions*, volume 10. Springer Science & Business Media, 2013.

[22] D Reiter, G Giesen, HJ Belitz, and W Eckstein. Database for recycling and penetration of neutral helium atoms in the boundary of a fusion plasma. Technical report, Forschungszentrum Juelich GmbH (Germany). Inst. fuer Plasmaphysik, 1992.

[23] Ursel Fantz, D Reiter, Bernd Heger, and D Coster. Hydrogen molecules in the divertor of asdex upgrade. *Journal of Nuclear Materials*, 290:367–373, 2001.

[24] V Kotov, D Reiter, RA Pitts, S Jachmich, A Huber, DP Coster, JET-EFDA contributors, et al. Numerical modelling of high density jet divertor plasma with the solps4. 2 (b2-eirene) code. *Plasma physics and controlled fusion*, 50(10):105012, 2008.

[25] Yulin Zhou, Benjamin Dudson, Fulvio Militello, Kevin Verhaegh, and Omkar Myatra. Investigation of the role of hydrogen molecules in 1d simulation of divertor detachment. *Plasma Physics and Controlled Fusion*, 64(6):065006, 2022.

[26] F Cianfrani, D Borodin, U Fantz, M Groth, A Holm, D Wünderlich, and P Boerner. Collisional-radiative model for transport simulations of neutrals in detached conditions. In *48th EPS Conference on Plasma Physics*, 2022.